

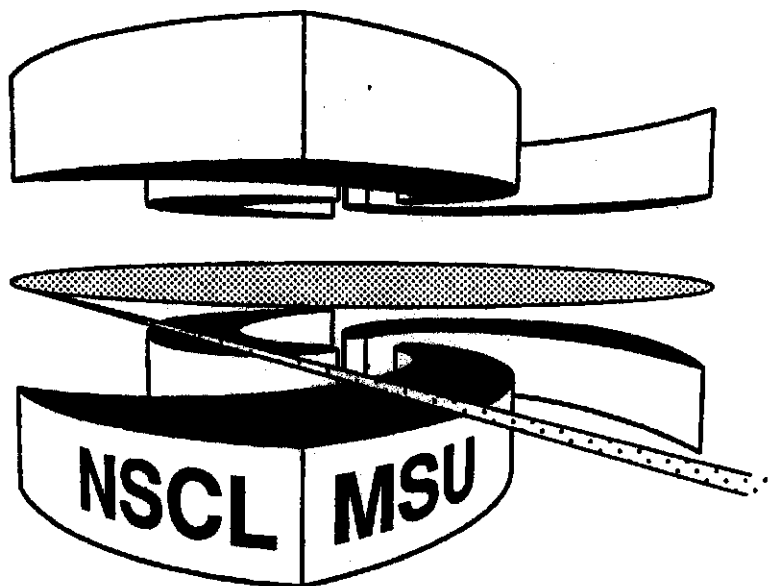


Michigan State University

National Superconducting Cyclotron Laboratory

**CANCER DETECTION VIA DETERMINATION OF
FRACTAL CELL DIMENSION**

WOLFGANG BAUER and CHARLES D. MACKENZIE



MSUCL-980

JULY 1995

Cancer Detection via Determination of Fractal Cell Dimension

Wolfgang Bauer

Department Of Physics and Astronomy and National Superconducting Cyclotron Laboratory, Michigan State University, East Lansing, MI 48824-1321, USA

Charles D. Mackenzie

Department of Pathology, Michigan State University, East Lansing, MI 48824, USA

We utilize the fractal dimension of the perimeter surface of cell sections **as a** new observable to characterize cells of different types. We propose that it is possible to distinguish **cancerous** from healthy **cells** with the aid of this new approach. **As a** first application we show that it is possible to perform **this** distinction between patients with hairy-cell **lymphocytic** leukemia and those with normal blood lymphocytes.

87.10.+e

In the final diagnosis of **neoplasia** the pathologist generally **relies** on the qualitative and empirical parameters of the cells in biopsies or cytological preparations. These experiential approaches have been aided by morphometric methods, such **as** determination of surface area, volume, axes ratios, estimation of population density, and other methods derived from basically Euclidian geometry [1], to enhance the examination of the internal components such **as** the nucleus, number of nucleoli, amount of **chromatin**, nuclear membrane abnormalities, together with perturbation of the **cytoplasmic** membrane, and degree of differentiation.

In mathematics and the physical sciences, it **has** been known since the turn of the century that classical Euclidian concepts, such **as** perimeter length, surface **area**, or volume, do not yield finite **answers** for certain objects. The earliest and probably most famous example **is** Koch's Snowflake [2] with infinite perimeter surface length and finite area. A similar problem is encountered when trying to **measure** the coastal length of **a** country like Great Britain, for example. There one finds that the answer depends on the size ϵ of **the** yardstick one is using, and that it diverges to infinity **as** the size of the yardstick approaches 0 [3]. In order to describe **this** kind of complexity found in nature, **Mandelbrot** developed the concept of fractal geometry [4]. He introduced the fractal dimension **as a** more convenient ways to parametrize the surface, $L(\epsilon) \sim F \epsilon^{1-d}$, where d is the fractal **Hausdorff** dimension.

In biology and medicine, **fractals** are just now beginning to have first applications [5,6]. Recently studied have been the shape of neurons in vertebrate central nervous systems [7], the frequency spectrum in human heartbeats [8], vascular and airway systems [9], brain surface [10], **trabecular** bone [11] and pathological entities such **as** **colorectal** polyps [12], or epithelial tissues in the oral cavity [13].

Fractals have also been utilized at the cell and sub-cellular level. The anatomical outline of **neuronal** cells [16], such **as** glia [17] and retinal cells [18] have been compared, and **so** has the nuclear outline of cervical epithelial cells [19] for cancerous changes. Surface receptor localization [20] and changes in **cytoplasmic** components such **as** **cytoskeleton** [21] and the nucleus of other cell types **has** revealed functional correlates.

In this current study we focus on the use of **fractals** at the cellular level. **In** the following we describe our method of extraction of fractal dimensions for biological cell samples [22]. We illustrate the method by showing the results of the different steps on a human lymphocyte **affected** by hairy-cell leukemia. However, the method is general and can be used on **many** types of cells or organisms such **as** protozoa and bacteria.

We start by obtaining an electron **microscope** image of **a** cell section (Fig. 1a). This image is digitized in 256 gray-levels at fairly high pixel resolutions. The image shown in Fig. 1a contains 750×675 pixels. By compiling grey level distribution histograms, one is able to automatically set **grey** level thresholds for the cell membrane and the cell nucleus. In Fig. 2 we show the **grey** level distribution for the digitized image of Fig. 1a. There **are** two local minima visible. The lower of these two minima corresponds to the threshold for the cell membrane, the object of interest here. The long vertical line corresponds to a **grey** level of 80, **chosen** for this particular cell. However, the exact choice (within ± 5) of the threshold value is relatively unimportant. We have investigated the sensitivity of our final results to the threshold value and find only **a** weak dependence over this range.

In the next **processing** step, every pixel with **grey** level above the threshold value is assigned black, and everyone below white. This results in the picture shown in Fig. 1b. One **can** now already **see a** rough image of the cell section's surface. However, there are small inclusions inside the cell which now appear **as** white spots, but upon examination of Fig. 1a clearly should belong to the cell. In the same way, there is extraneous **extracellular** material (seen **as** black aggregates), mainly from proteins in the solution, which clearly don't belong to the cell, either. These small black and white spots have to be removed for us to obtain meaningful information on the surface of the cell.

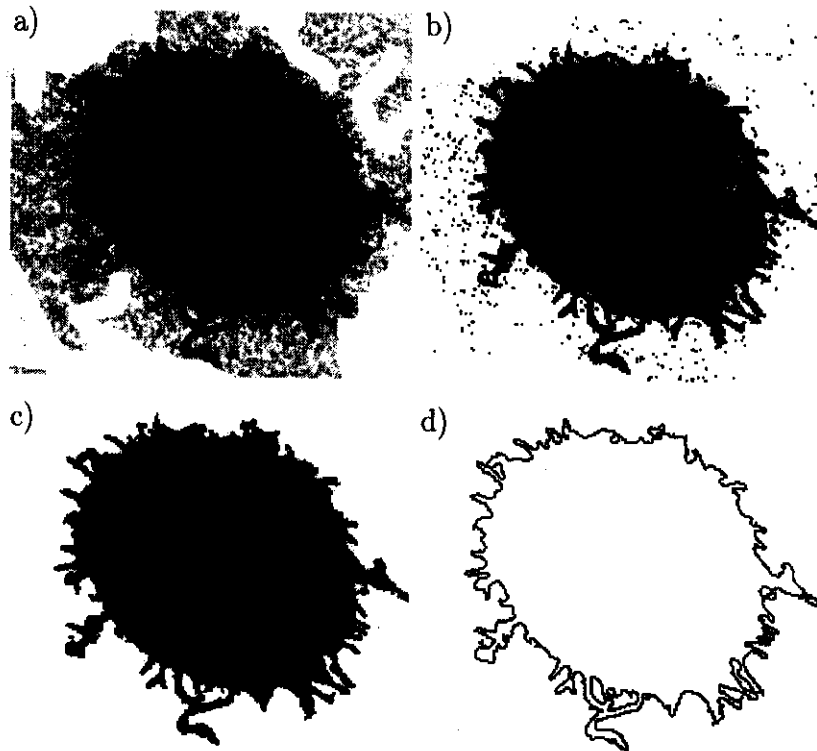


FIG. 1. a) Electron microscope image of a section of a human lymphocyte, affected with hairy-cell leukemia, digitized with 256 grey levels. b) Black/white representation of (a) with a grey level threshold set at 80. c) Image after application of our small-cluster removal algorithm. d) Perimeter surface of the image, obtained by taking derivatives in x and y directions.

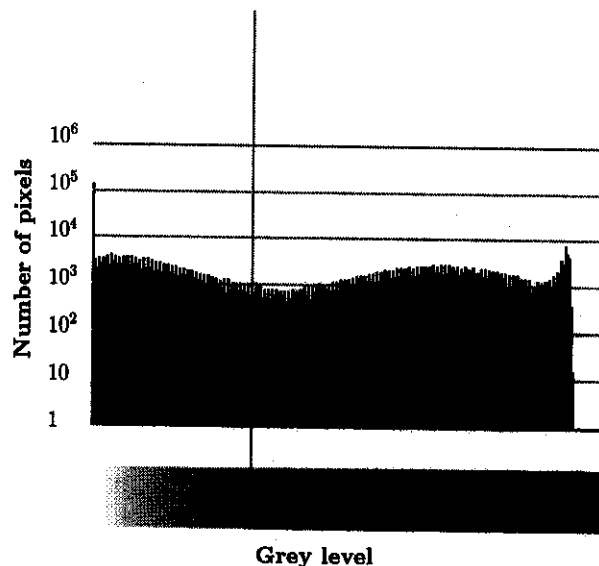


FIG. 2. Grey level distribution for image shown in Fig. 1a.

Conventional speckle removal algorithms do not work in our case, because techniques like neighboring-pixel-averaging tend to smoothen the true cell surface as well, often resulting in a changed fractal dimension. Fortunately, we were able to utilize a cluster-recognition algorithm, developed by one of us to identify fragments in nuclear [23] and bucky-ball [24] fragmentation. This is yet another example where basic research in one field has lead to a completely unexpected applied spinoff in another. With this algorithm we identify all clusters below a minimum size and invert

their grey level value. This minimum size was universally chosen to be 300 pixels in all cells processed by us. We have varied this parameter and find only minimal influence on our final results over a reasonable range (100 – 500). The output of this algorithm is shown in Fig. 1c. One can clearly see that all speckles have been successfully removed, and that the overall shape of the surface was not altered in the process.

It is now straightforward to obtain pixels on the surface of the cell section by taking partial derivatives in the x and y coordinates. These derivatives are surface-peaked and have a value of 0 elsewhere. The result of this procedure is shown in Fig. 1d, where the surface is now represented as a black line on an otherwise white background. By comparing Fig. 1d with Fig. 1a, one can see that the automated surface recognition procedure outlined here does the job rather well.

We now determine the fractal dimension, d , of the surface by utilizing the box-counting method. It was shown that this method yields quantitative agreement with the line-segment method discussed above [25]. In the box-counting method, one utilizes the definition of the Hausdorff-dimension, where the number, $N(\xi)$, of squares of side-length ξ needed to cover a set increases like $N(\xi) \propto \xi^{-d}$ for $\xi \rightarrow 0$ for a set of fractal Hausdorff dimension d . One then can theoretically obtain the fractal dimension from $d = -\log[N(\xi_1)/N(\xi_2)]/\log[\xi_1/\xi_2]$.

However, in practice there are some difficulties associated with arbitrarily choosing ξ_1 and ξ_2 . We chose our sidelength as integer powers of 2, $\xi_i = 2^{-i}$. For a too small value of l , $N(\xi_i)$ will increase like for a 2-dimensional set. For a too large value of l , $N(\xi_i)$ will approach a constant, the total number of pixels on the surface. This asymptotic limit for sets of finite numbers of points has been studied, and methods have been devised to correct for this effect [26]. However, in our case an approximate determination of d within ± 0.03 is fully sufficient, and we found that a linear regression fit for the l -values in the range 3 to 6 (corresponding to a ξ -range between 1/8 and 1/64 and total numbers of boxes between 64 and 4096) yielded satisfactory results. In all cases considered, we obtained correlation coefficients of $1 - r < 10^{-2}$. We also tested our method on known fractals such as Koch's Snowflake and Sierpinsky's Carpet, and obtained the exact results to within the uncertainty specified above.

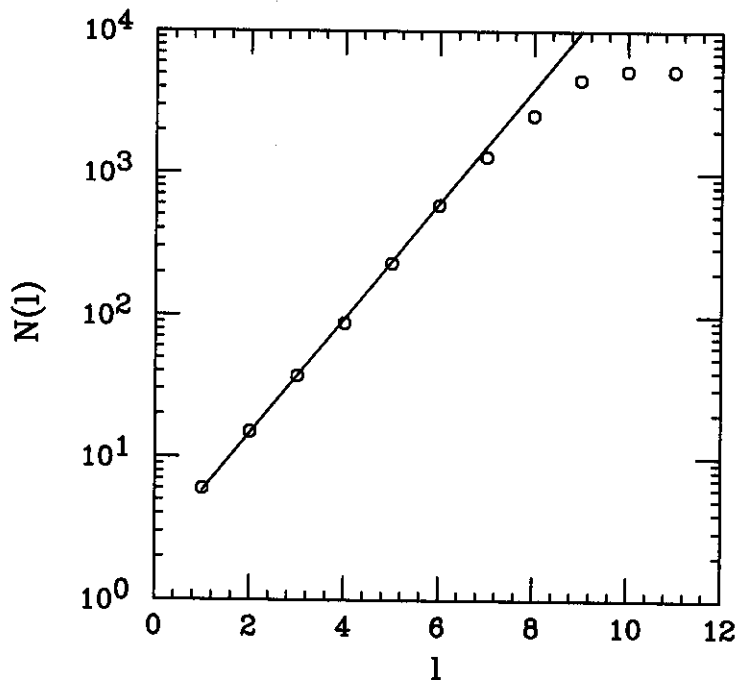


FIG. 3. Number of boxes touched by the perimeter surface of Fig. 1d. as a function of l , where the box side length is given by $s = 2^{-l}$. The straight line is a fit in the interval $l = [3, 6]$.

In Fig. 3, we show (circles) the results of our box-counting algorithm for the surface of the cell section as displayed in Fig. 1d. The total number of surface pixels happened to be 5297 in this case, a limit reached for $l = 10$. The power-law fit in the l -interval from 3 to 6 yields a fractal dimension of $d = 1.34$ (with a correlation coefficient of $r = 0.99975$) and is represented by the straight line.

With this method of determination of the fractal box-counting dimension of the surface of a cell section it is possible to derive a *quantitative* measure for the raggedness of cells or small biological organisms. We report here on

our initially most important result, the investigation of human blood lymphocytes affected by hairy-cell leukemia.

To perform our test, we obtained archive electronmicrographs of white blood cell preparations of two patients who died of hairy-cell leukemia. As controls, we also processed white blood cells of healthy patients. In each group patient we examined samples of about 100 cells, for which we determined the fractal dimension individually. The result of applying our method to these cell samples is shown in Fig. 4. The number of cells with fractal dimension d_{eff} are binned in (area normalized) histograms and displayed as a function of d_{eff} .

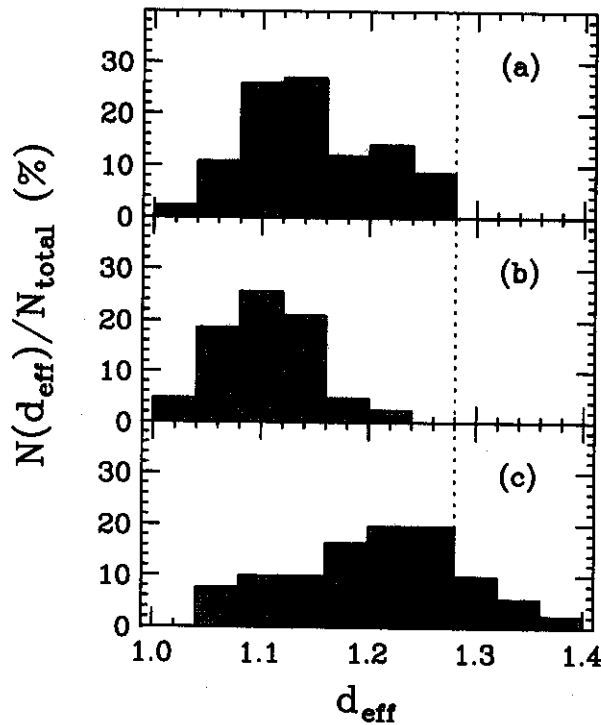


FIG. 4. Histograms of fractal dimensions of sections of individual cells: a) White blood cells of healthy persons; (b) Lymphocytes of healthy persons; (c) Lymphocytes of hairy cell leukemia patients. The dotted vertical line indicates a fractal dimension of 1.28, a value which is surpassed only by cells from the cancer patients.

In Fig. 4a we show the distribution of white blood cells for the healthy patients. Hairy-cell leukemia is a form of lymphocytic neoplasia that produces varying proportions of circulating neoplastic cells characterized by their morphologically altered cytoplasmic membranes, which carry considerably more surface projections (pseudopods) than do normal healthy lymphocytes. However, other normal cells in blood, e.g. neutrophils and other granulocytes, which may constitute 50% or more of the sample, can also have a rough (“hairy”) surface. One can discriminate against them by examining deformation of the cell nucleus. Taking this criterion into account, one arrives at the histogram shown in Fig. 4b, the distribution of fractal dimensions for healthy lymphocytes.

In Fig. 4c we show the distribution obtained from the lymphocytes of the cancer patients. The dotted vertical line indicates a fractal dimension of 1.28. None of the cells of the healthy patients had a fractal dimension larger than this value, whereas a large percentage of the cells of the cancer patients had $d > 1.28$. The difference between the fractal dimension distributions for healthy and hairy-cell leukemic patient lymphocytes is obvious.

In summary, we have used the concept of fractal dimensional analysis of surfaces of individual cells. We have shown on the example of a white human blood cell how our method works, and that a meaningful extraction of a fractal dimension is possible by using automated computer procedures. In this first exploratory study we have presented a classification of cell samples in terms of a fractal dimension histogram of cells. We showed that it is possible to distinguish between healthy persons and hairy-cell leukemia cancer patients on the basis of our method.

In the future we see two direct application of our method. First, one can envision our system as a diagnostic aid for the practicing pathologist. With it a technician can use our system on a very large cell sample, picking out only the most interesting diagnostically relevant individual cells for visual inspection by the pathologist. This is possible

at the present stage of development. A second, completely automated, application should also be possible. For this, however, carefully controlled, double-blind clinical studies are necessary. We plan to start this in the near future.

We expect that our method will also be readily applicable to a host of other cancers, most prominently breast cancer. We speculate that there might exist a connection between shape change, i.e. change in fractal dimension, and metastasis. If this holds true, then our method could be used for early detection.

-
- [1] W.A. Aherne and M.S. Dunnill, *Morphometry* (Edward Arnold Publishers, London, 1982).
 - [2] H. von Koch, *Arkiv för Matematik* **1**, 681 (1904).
 - [3] L.F. Richardson, *General Systems Yearbook* **6**, 139-187 (1961).
 - [4] B. Mandelbrot, *The fractal geometry of nature* (W.H. Freeman, New York, 1977).
 - [5] B.J. West, *Fractal Physiology and Chaos in Medicine* (World Scientific, Singapore, 1990).
 - [6] A. Bunde and S. Havlin, *Fractals in Science* (Springer, Heidelberg, 1994).
 - [7] T.G. Smith, W.B. Marks, G.D. Lange, W.H. Sheriff Jr., and E.A. Neale, *J. Neuroscience Methods* **27**, 173 (1989).
 - [8] C.-K. Peng, J.E. Mietus, J.M. Hausdorff, S. Havlin, H.E. Stanley, A.L. Goldberger, *Phys. Rev. Lett.* **70**, 1343 (1993).
 - [9] R.Z. Gan, Y. Tian, R.T. Yen, G.S. Kassab, *Journal of Applied Physiology* **75**, 432 (1993).
 - [10] C.E. Priebe, J.I. Solka, R.A. Lorey, G.W. Rogers, W.L. Poston, M. Kallergi, W. Qian, L.P. Clarke, R.A. Clark, *Cancer Letters* **77**, 183 (1994).
 - [11] J.C. Buckland-Wright, J.A. Lynch, J. Rymer, I. Fogelman, *Calcif. Tissue. Int.* **54**, 106 (1994).
 - [12] S.S. Cross, J.P. Bury, P.B. Silcocks, T.J. Stephenson, D.W. Cotton, *Journal of Pathology* **172**, 317 (1994).
 - [13] G. Landini, J.W. Rippin, *Anal. Quant. Cytol. Histol.* **15**, 144 (1993).
 - [14] R. Thibert, B. Dubuc, M. Dufour, R. Tawashi, *Scanning Microscopy* **7**, 555 (1993).
 - [15] M. Battaglia-Parodi, D.D. Giusto, *Ophthalmic Research* **25**, 307 (1993).
 - [16] S. Traverso, R. Morchio, G. Tamone, *Riv. Biol.* **85**, 405 (1992).
 - [17] T.G. Smith Jr., T.N. Behar, *Brain Research* **634**, 181 (1994).
 - [18] H. Holb, E. Fernandez, J. Schouten, P. Ahnelt, K.A. Linberg, S.K. Fisher, *J. Comp. Neurol.* **343**, 370 (1994).
 - [19] C. MacAulay, B. Palcic, *Anal. Quant. Cytol. Histol.* **12**, 394 (1990).
 - [20] A. Sadana, A. Madagula, *Biosens. Bioelectron.* **9**, 45 (1994).
 - [21] M.A. Aon, S. Cortassa, *FEBS-Letters* **344**, 1 (1994).
 - [22] W. Bauer and C.D. Mackenzie, "Method and System For Detection of Biological Materials", Michigan State University 4.1-128 (ID 94-030), US patent applied for.
 - [23] W. Bauer, D.R. Dean, U. Mosel, and U. Post, *Phys. Lett.* **150B**, 53 (1985); W. Bauer, *Phys. Rev. C* **38**, 1927 (1988).
 - [24] T. Le Brun, H.G. Berry, S. Cheng, R.W. Dunford, H. Esbensen, D.S. Gemmell, E.P. Kantor, and W. Bauer, *Phys. Rev. Lett.* **72**, 3965 (1994).
 - [25] J. Feder, *Fractals* (Plenum Press, New York, 1988).
 - [26] P. Grassberger, *Phys. Lett.* **97A**, 224 (1983).